frontiers in Earth Science

ORIGINAL RESEARCH
published: 30 April 2021
doi: 10.3389/feart.2021.675726

Reconstructing Nitrogen Sources to Earth's Earliest Biosphere at 3.7 Ga

Eva E. Stüeken[1], Toby Boocock[1], Kristoffer Szilas[2], Sami Mikhail[1] and Nicholas J. Gardiner[1,3]*

[1] School of Earth and Environmental Sciences, University of St Andrews, St Andrews, United Kingdom, [2] Department of Geosciences and Natural Resource Management, University of Copenhagen, Copenhagen K, Denmark, [3] School of Earth, Atmosphere and Environment, Monash University, Melbourne, VIC, Australia

Earth's sedimentary record has preserved evidence of life in rocks of low metamorphic grade back to about 3.2–3.5 billion years ago (Ga). These lines of evidence include information about specific biological metabolisms, permitting the reconstruction of global biogeochemical cycles in the early Archean. Prior to 3.5 Ga, the geological record is severely compromised by pervasive physical and chemical alteration, such as amphibolite-granulite facies metamorphic overprinting. Despite this alteration, evidence of biogenic organic matter is preserved in rare localities, including meta-turbidites from the 3.8 to 3.7 Ga Isua Supracrustal Belt, Western Greenland. But detailed insights into metabolic strategies and nutrient sources during the time of deposition of these Eoarchean meta-sedimentary rocks are lacking. Here we revisit the Isua meta-turbidites and provide new data for metal abundances as well as organic carbon and nitrogen isotope values. Our results reveal mixing between authigenic and detrital nitrogen phases with the authigenic phase likely fractionated by metamorphic degassing. Rayleigh fractionation models of these 3.7 Ga samples indicate pre-metamorphic $\delta^{15}N$ values of between −1 and −10‰. The most plausible initial values are below −5‰, in agreement with a prior study. While the upper endmember of −1‰ could indicate biological N_2 fixation at 3.7 Ga, the more plausible lighter values may point toward a distinct biogeochemical nitrogen cycle at that time, relative to the rest of Earth's history. In light of recent experimental and phylogenetic data aligned with observations from the modern atmosphere, we tentatively conclude that lightning and/or high-energy photochemical reactions in the early atmosphere may have contributed isotopically light nitrogen to surface environment(s) preserved in the Isua turbidites. In this case, recycling of Eoarchean sediments may have led to the isotopically light composition of the Earth's upper mantle dating back to at least 3.2 Ga.

Keywords: Eoarchean, Isua, metamorphism, lightning, nitrogen isotopes

OPEN ACCESS

Edited by:
Naohiko Ohkouchi, Japan Agency for Marine-Earth Science and Technology (JAMSTEC), Japan

Reviewed by:
Tsuyoshi Komiya, The University of Tokyo, Japan
Huan Cui, Université de Paris, France

****Correspondence:***
Eva E. Stüeken
ees4@st-andrews.ac.uk

Specialty section:
This article was submitted to Biogeoscience, a section of the journal Frontiers in Earth Science

Received: *03 March 2021*
Accepted: *06 April 2021*
Published: *30 April 2021*

Citation:
Stüeken EE, Boocock T, Szilas K, Mikhail S and Gardiner NJ (2021) Reconstructing Nitrogen Sources to Earth's Earliest Biosphere at 3.7 Ga. Front. Earth Sci. 9:675726. doi: 10.3389/feart.2021.675726

INTRODUCTION

Signatures of life on Earth have previously been identified in some of the oldest rocks on Earth, dating back to almost 4 billion years ago (reviewed by Lepot, 2020). These signatures include carbon isotope values indicative of biological CO_2 fixation (Rosing, 1999), which today plays a major role in the global carbon cycle and may have done so for most of Earth's history (Schidlowski, 2001). In

contrast, the antiquity of other metabolic pathways (e.g., nitrogen, phosphorus, or sulfur uptake) is more elusive, because metamorphic alteration severely impacts our ability to extract primary information from the oldest paleobiological records. For example, in the case of nitrogen, evidence of biological N_2 fixation has so far been taken back to ca. 3.2 Ga (Beaumont and Robert, 1999; Stüeken et al., 2015; Homann et al., 2018; Koehler et al., 2019a), though phylogenetic data suggest that this metabolism already existed in the last universal common ancestor, possibly as early as 3.8 Ga (Weiss et al., 2016).

A widely used geochemical tool to reconstruct nitrogen cycling in deep time are nitrogen isotopes (Ader et al., 2016; Stüeken et al., 2016); however, primary isotopic values are easily perturbed during metamorphism at greenschist facies grades and above (reviewed by Thomazo and Papineau, 2013), which prohibits detecting specific nitrogen metabolisms in Eoarchean rocks. A lack of knowledge about the primary $\delta^{15}N$ composition of the sedimentary cover in the earliest intervals of Earth's history also has important implications for our understanding of the geological nitrogen cycle through time. In the modern Earth system, biogenic nitrogen buried in sediments can be subducted into Earth's mantle in significant quantities, which, if true in the past, may have had important implications on the evolution of atmospheric N_2 pressure, and therefore planetary habitability, over billion-year timescales (e.g., Mikhail and Sverjensky, 2014; Barry and Hilton, 2016; Busigny et al., 2019). However, constraining the onset of biogenic nitrogen burial requires better constraints on the biogenic $\delta^{15}N$ endmember in the past, because this endmember is required to distinguish sedimentary from mantle-derived nitrogen sources. In short, there is a significant need to determine the primary $\delta^{15}N$ composition of Eoarchean sediments.

To address this knowledge gap, we revisited some of the world's oldest metasedimentary rocks located in the Eoarchean Isua Supracrustal Belt, West Greenland, where previous studies documented graphitic schists with $\delta^{13}C$ values and elemental compositions diagnostic of a biogenic origin (Rosing, 1999; Hassenkam et al., 2017). We analyzed these rocks for nitrogen isotopes and abundances and determined a best-estimate initial composition via a Rayleigh fractionation model. Albeit indirect, our approach allows us to place new constraints on plausible nitrogen sources to Earth's earliest biosphere.

GEOLOGICAL SETTING

The Eoarchean Isua Supracrustal Belt (ISB) of South Western Greenland (**Figure 1**) represents the oldest meta-sedimentary and meta-volcanic sequence on Earth and has therefore been intensively studied since the 1970s (e.g., Moorbath et al., 1973; Moorbath et al., 1975; Baadsgaard et al., 1984; Nutman and Friend, 2009; Nutman et al., 2019). The ISB is hosted by the >3.6 Ga Itsaq Gneiss Complex, which is the world's most extensive domain of Early Archean crustal rocks, and forms part of the North Atlantic Craton (Nutman et al., 1996). This craton represents the amalgamation of several distinct tectonomagmatic crustal blocks, and therefore experienced a long and complex deformation and thermal history (Friend and Nutman, 2019). The complex nature of the Itsaq Gneiss Complex and the ISB in particular, complicates the interpretation of the protoliths and the degree to which these rocks preserves primary features (Myers, 2001; Whitehouse et al., 2009).

The metamorphic mineral assemblages recorded by the ISB documents a polymetamorphic history with thermal events in both the early and late Archean (Boak and Dymek, 1982; Rollinson, 2002; Rollinson, 2003). Rocks with garnet-hornblende-plagioclase-quartz and garnet–epidote–biotite–muscovite–quartz–graphite assemblages (Boak and Dymek, 1982; Rosing, 1999) support a prograde peak metamorphic temperature of ∼550°C and pressure of ∼5 to 7 kbar (∼15 km burial depth) before 3.6 Ga (Boak and Dymek, 1982). Recently it has been proposed that contrasting metamorphic T/P regimes are recorded in the ISB, resembling modern paired metamorphic belts, which support the hypothesis that the ISB formed at a convergent margin with peak pressure above 1 GPa (Nutman et al., 2020; Guotana, submitted). Thus, overwhelmingly, the ISB has been interpreted in the context of having formed by subduction zone processes (Hanmer and Greene, 2002; Polat et al., 2002; Jenner et al., 2009; Hoffmann et al., 2010). However, recent studies questioned this long-held model based on a new structural analysis of the ISB (Webb et al., 2020), and due to a detailed investigation of the metamorphic regimes that ISB experienced (Ramírez-Salazar et al., 2021). The latter authors found evidence for three distinct metamorphic events (M_i) with peak conditions of 550–600°C and 0.5–0.7 GPa at M_1, <540°C and <0.5 GPa at M_2, and finally low temperature retrogression of <500°C at M_3. M_1 and M_2 likely occurred at >3.5 and >2.9 Ga, whereas M_3 is currently not well-constrained.

For this study, we focused on a succession of metamorphosed siliciclastic sedimentary rocks (**Figure 2**) that have previously been interpreted as a meta-turbidite and yielded organic carbon isotope values indicative of biogenic organic matter (Nutman et al., 1984; Rosing et al., 1996; Rosing, 1999). The succession is approximately 50 m thick; individual beds are 10–70 cm in thickness and defined by sharp bases and normal grading. The meta-turbidite rests on top of meta-basalts with pillow structures. Prior work on U abundances was interpreted as evidence of oxic conditions conducive of U mobilization in the depositional basin (Rosing and Frei, 2004). The U would then have been trapped in locally anoxic sediments represented by roughly 10 cm-thick organic-rich slates of the turbidite succession (**Figure 2**). The U abundance data were thus used to infer the presence of oxygenic photosynthetic bacteria at 3.7 Ga. In this study, we sampled the same slate horizons for analyses of organic carbon and nitrogen isotopes as well as major and minor element abundances.

METHODS

The rock samples were cut with a water-cooled diamond saw to remove any weathered surfaces. The interiors were then hammered into sub-cm sized chips with a steel pestle on a steel plate, and the chips were subsequently washed with methanol

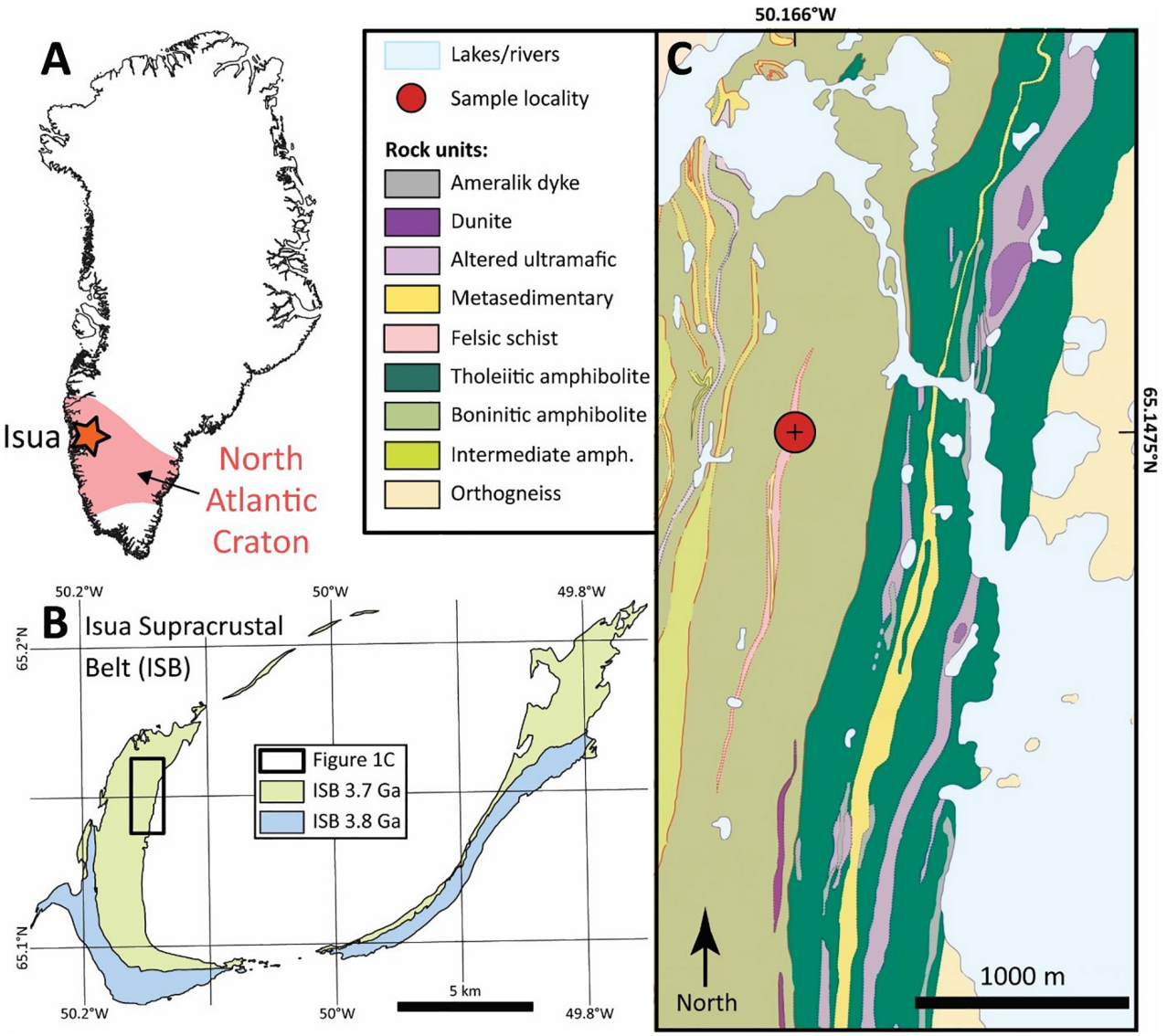

FIGURE 1 | Geological map of the Isua Supracrustal Belt. **(A)** Shows the extent of the Archean North Atlantic Craton in Greenland, with the position of Isua marked by the star. **(B)** Overview map of the Isua Supracrustal Belt, with the two distinct sequences shown in blue and green colors. The study area is outlined by the box. **(C)** Detailed geological map of the locality from which the samples of the present study were collected. Modified after and Nutman and Friend (2009) and Waterton (submitted).

(reagent grade), 1M HCl (reagent grade) and 18 MΩ/cm^{-1} DI-water. The clean chips were dried overnight in an oven at 70°C and then pulverized in an agate ball mill. The milling vessels were cleaned with pre-combusted silica sand (500°C overnight) in between samples, wiped with DI-water and methanol, and blow-dried with compressed air. The rock powders were stored in pre-combusted scintillation vials. Prior to isotopic analyses, an aliquot of ∼0.5 g of each sample was decarbonated with 2M HCl in pre-combusted Pyrex centrifuge tubes and then washed three times with DI-water. The decarbonated residue was dried in a closed oven at 70°C. For organic carbon and total sulfur analyses, around 50 mg of each decarbonated powder were weighed into tin capsules (8 × 5 mm^2 in cross section, Thermo Fisher), mixed with ∼5 mg of V_2O_5 (Elemental Microanalysis), and analyzed by flash-combustion with an elemental analyzer (EA IsoLink, Thermo Fisher) coupled to a gas source mass spectrometer (MAT253, Thermo Fisher) via a ConFlo IV (Thermo Fisher). The data were calibrated with the international reference materials USGS-40 and USGS-41 for carbon and IAEA-S2 and IAEA-S3 for sulfur. Results are expressed in standard delta notation (δ [‰] = [($R_{sample}/R_{standard}$) − 1] × 1000), where R = $^{13}C/^{12}C$ for $\delta^{13}C$ and R = $^{34}S/^{32}S$ for $\delta^{34}S$. Reference standards are VPDB for carbon and VCDT for sulfur. The average reproducibility of replicate analyses of the same sample was ±0.4‰ for $\delta^{13}C$ and ±0.6‰ for $\delta^{34}S$. Peak areas were calibrated for total organic carbon (TOC) and total sulfur (TS) abundances.

FIGURE 2 | Photo of the main outcrop of the turbidite locality from which the studied samples were taken, which is the same locality that was documented by Rosing (1999). The graphitic slate is the obvious dark layer in the middle, with the proposed meta-turbidites on either side of it displaying gradational lamination. This outcrop is a protected site, and hence the samples for this study are from the continuation of the strata a couple of meters above and behind this rock face. Backpack for scale.

For nitrogen abundance and isotopes, analyses were done by offline combustion, which allows accurate isotopic analyses down to low nitrogen abundances (<10 ppm) in hard-to-combust silicate phases (Boocock et al., 2020). Quartz glass tubes were cleaned by combustion at 1,000°C for >6 h before use. Similarly, CuO wire was prepared by pre-combustion at 800°C for >6 h to ensure that any adsorbed N_2 impurities were volatilized before introducing samples, hence minimizing the reagent nitrogen blank. Approximately 300 mg of sample powder were then weighed into the quartz tubes and mixed with 0.5 g of CuO wire. Sample tubes were attached to a custom-built vacuum line and evacuated overnight to $<10^{-5}$ mbar. During the evacuation, the samples and quartz tubes were heated to 120°C to remove adsorbed moisture and volatile contaminants. The next day, the quartz tubes were sealed with an oxy-acetylene blow torch. Sealed evacuated tubes containing sample powders were then placed into a muffle furnace at 950°C for 4 h, followed by 2 h at 600°C and slow cooling to room temperature. This procedure converts all rock-bound nitrogen into N_2 gas. The gas samples were analyzed with a tube cracker attached to the same ConFlo and mass spectrometer as the elemental analyzer used for carbon and sulfur analyses. Analyses were calibrated with USGS-61 and USGS-62 and are reported as $\delta^{15}N = [(^{15}N/^{14}N)_{sample}/(^{15}N/^{14}N)_{air}) - 1] \times 1000$. Procedural blanks were measured throughout the analytical campaign and had an average composition of 20.1 nmol total N at with a $\delta^{15}N$ value of $-2.1 \pm 0.9‰$. This average value was subtracted from all standard and sample data. To assess analytical accuracy, we analyzed three aliquots of BHVO-2 and obtained an isotopic value of $+2.3 \pm 0.3‰$ and a total nitrogen abundance of 20.8 ± 0.9 ppm, which agrees well with previous studies (Feng et al., 2018; Boocock et al., 2020).

For major and minor elemental abundance analyses, untreated rock powders were sent to Australian Laboratory Services in Dublin. Here, samples were dissolved in HF, $HClO_4$, HNO_3 and HCl and analyzed by ICP-MS and ICP-OES. The reproducibility (1SD) of major elements was generally better than 4% (relative error) and better than 11% for minor elements.

RESULTS

The results are summarized in **Tables 1**, **2**. Eight of the nine samples contain moderate amounts of organic carbon (TOC = 0.05 – 0.80 wt.%, **Figure 3B**) and show a tight distribution of carbon isotope values around a mean of $-18.1 \pm 0.5‰$ (1SD), which is in good agreement with previous measurements on the same stratigraphic unit (-14 to $-20‰$, Rosing, 1999). The remaining sample had too little TOC (0.003 wt.%) for reliable carbon isotope determinations. Total nitrogen abundances (TN) and $\delta^{15}N$ values show two populations, one with low abundances (4.8 ± 1.3 ppm) and $\delta^{15}N$ around $+2.3 \pm 0.7‰$ and a second with slightly higher abundances (26.2 ± 6.4 ppm) and an average $\delta^{15}N$ of $+6.1 \pm 0.7‰$ (**Figure 3A**). TN and $\delta^{15}N$ thus positively correlate with each other, which is opposite to the negative correlation that would be expected from metamorphic devolatilization of a homogeneous starting composition (Haendel et al., 1986). To assess the degree of lab-derived contamination, pure minerals (quartz, plagioclase, orthoclase, biotite, muscovite, kaolinite) and baked silica sand were processed through the same rock crushing and

TABLE 1 | Major and minor element abundances.

	Al	Ca	Ce	Co	Cr	Cu	Fe	K	La	Mg	Mn	Mo	Na	Ni	P	Pb	Sc	Th	Ti	U	V	Y	Zn	Zr
	%	%	ppm	ppm	ppm	ppm	%	%	ppm	%	ppm	ppm	%	ppm	ppm	ppm	ppm	ppm	%	ppm	ppm	ppm	ppm	ppm
208288	6.9	0.82	4.18	14.3	51	59.6	4.68	0.85	1.7	1.07	565	0.36	2.58	88.5	310	1.7	6.5	2.52	0.221	0.6	35	7.3	36	87
208289	8.22	1.1	30.9	16.9	19	0.2	4.92	0.62	13	1.7	777	0.02*	4.29	24.7	440	2.1	9.7	3.2	0.365	0.7	70	10.5	95	119
208290	6.33	2.37	7.95	3.5	45	4.1	2.03	3.21	3.8	0.52	1,290	0.07	0.12	16.4	330	1.4	8.1	2.02	0.234	0.6	47	7.7	18	76
208291	8.86	2.93	20.4	9.4	89	0.1*	4.75	3.58	9.1	1.42	1,290	0.02*	0.46	66.9	470	2.4	11.9	3.08	0.36	0.7	72	9.8	46	94
208292	9.23	1.47	29	9.3	97	0.1*	5.49	3.83	12.1	1.69	1,400	0.02*	0.35	71.5	490	1.7	12.3	3.44	0.387	0.7	78	9.8	54	119
208293	7.83	2.78	22.7	12.6	123	0.1*	4.51	2.34	9.1	1.86	1,720	0.07	1.44	101	440	2.7	12	2.52	0.349	0.7	75	9.5	54	115
208294	5.92	0.83	4.34	21.7	41	80.9	3.83	0.59	1.7	0.76	428	0.46	2.76	101.5	350	1.6	5	2.66	0.196	0.9	22	5.7	28	110
208295	9.04	2.85	24.9	11.3	84	0.1*	7.45	4	10.1	1.04	929	0.09	0.39	66	400	3.3	9.4	2.47	0.319	0.7	65	10	66	32
208296	9.19	0.4	6.07	15.6	97	8.5	8.37	2.31	2.2	1.68	2,510	0.14	1.2	116	440	1.1	10.8	3.29	0.338	0.7	66	20.6	59	115

** = measurements were below detection limit and are reported as 0.5 × the limit of detection.*

TABLE 2 | Organic carbon, total nitrogen and total sulfur data.

	TOC	$\delta^{13}C$	TN	$\delta^{15}N$	TS	$\delta^{34}S$	C/N
	(wt.%)	(‰)	(ppm)	(‰)	(wt.%)	(‰)	(mol/mol)
208288	0.323	−18.83	6.1	3.02	0.23	1.81	620
208289	0.003		3.4	1.75	0.00		10
208290	0.395	−17.54	25.1	5.89	0.01	−0.29	183
208291	0.117	−18.34	30.9	5.96	0.00		44
208292	0.119	−17.95	36.6	6.93	0.00		38
208293	0.045	−18.42	19.7	6.10	0.00		27
208294	0.622	−18.25	4.8	2.05	0.23	1.90	1509
208295	0.797	−17.41	23.4	6.75	0.00		397
208296	0.427	−18.05	21.6	5.06	0.00		230

decarbonation protocol and found to accumulate a maximum of 1 ppm N; some specimens lost N compared to a hand-crushed aliquot due to the washing step and acid-treatment of the rock powder (Stüeken et al., 2021). Hence contamination in the laboratory is not a major contributor of N to the samples. The covariance between TN and $\delta^{15}N$ is therefore indigenous to the rocks.

Molar ratios of organic carbon to total nitrogen (hereafter C/N) vary widely with C/N ratios from 10 to 1,509. TN is not correlated with TOC (r^2 = 0.01) but strongly correlated with potassium abundances (r^2 = 0.89) (**Figures 3C,D**), indicating that the nitrogen contained in these rocks is now mostly silicate-bound as opposed to organic-bound. Total sulfur concentrations range from 0.001 to 0.230 wt.%. Only three samples yielded enough sulfur for isotopic analyses and showed $\delta^{34}S$ values around a mean of +1.1 ± 1.2‰. Total sulfur is not correlated with TOC (**Figure 4A**) but covaries with Cu and Mo (**Figures 4B,D**), indicating that these metals are dominantly sulfide-bound. Molybdenum shows no correlation with TOC (**Figure 4C**), counter to what is observed in modern marine sediments (Wilde et al., 2004). Ratios of Ni/Co (mean 5.9 ± 2.1), Th/Sc (0.3 ± 0.1), Fe/Al (0.6 ± 0.2) and U/Th (0.3 ± 0.0) fall in between those of average upper continental crust (Rudnick and Gao, 2014), average oceanic crust (White and Klein, 2014), and average komatiite (Ptáček et al., 2020; **Figure 5**).

DISCUSSION

Sedimentary Provenance and Redox Conditions

Sedimentary provenance, mild hydrothermal alteration and metasomatism have affected the major and minor element distribution in these rocks, and therefore need to be addressed. Regarding sedimentary provenance, mapping has shown that the turbidites analyzed in this study sit on top of mafic volcanic rocks (Rosing et al., 1996), and our Th/Sc, U/Th and Fe/Al ratios are indeed consistent with a strong contribution of mafic detritus. These element ratios were selected because they have previously been shown to be good discriminators for distinguishing between mafic, ultramafic and felsic provenance (Ptáček et al., 2020). All three ratios fall in between those of average upper continental crust and average oceanic crust (Rudnick and Gao, 2014; White and Klein, 2014), which suggest mixing of material from sources of similar compositions. The relatively high Ni/Co ratios may further indicate contributions of ultramafic material, such as komatiite (**Figure 5A**), consistent with previous studies of other Archean siliciclastic rocks (Ptáček et al., 2020). This interpretation is overall in line with previous trace element work on metasedimentary rocks from the Isua Supracrustal Belt (Kamber et al., 2005).

In the case of U/Th and Fe/Al, input of mafic or ultramafic detritus has important implications for the utility of these elements as redox proxies. We briefly address this topic here, because previous work found geochemical evidence of biological oxygen production in rocks from this same geological unit (Rosing and Frei, 2004). A high Fe/Al ratio above ∼0.5 in sedimentary rocks, i.e., elevated relative to upper continental crust, is typically interpreted as evidence of anoxic conditions during the time of deposition that favored the accumulation of authigenic iron minerals, including sulfides, carbonates or oxides (Lyons and Severmann, 2006; Raiswell et al., 2019). However, in settings with significant contributions of iron-rich siliciclastic material or detrital iron sulfides or iron oxides, such as mafic rock-forming minerals and their weathering products, this empirically defined threshold is no longer applicable (Stüeken et al., 2017; Stüeken et al., 2020). It is therefore not possible to

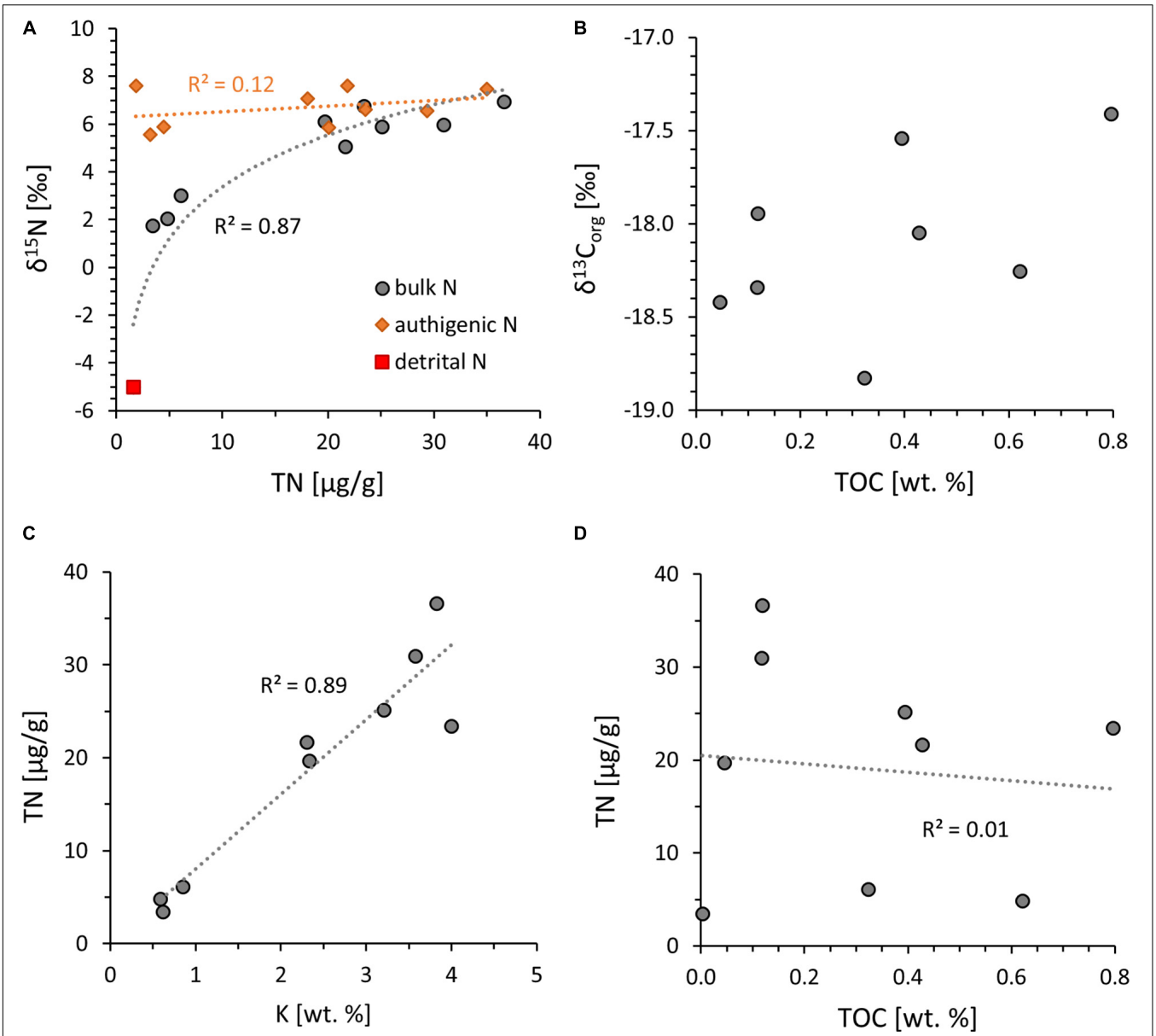

FIGURE 3 | Organic carbon and nitrogen data. **(A)** $\delta^{15}N$ vs. total nitrogen (TN). Gray circles = measured data; red square = assumed detrital endmember; orange diamonds = calculated authigenic nitrogen component (see text for details). **(B)** $\delta^{13}C_{org}$ vs. total organic carbon (TOC). **(C)** Measured TN vs. K with strong covariance, indicating that most N is now bound to potassic minerals. **(D)** TN vs. TOC, showing no correlation, suggesting that only minor amounts of nitrogen are bound to organic matter.

infer redox conditions during the time of deposition on the basis on Fe/Al ratios. Other commonly used redox proxies include Mo abundances and U/Th ratios (Tribovillard et al., 2006). Both Mo(VI) and U(VI) are soluble under oxic conditions and can thus become enriched in anoxic sediments as Mo(IV) and U(IV), respectively. However, we find no evidence for enrichments in either of these proxies above the level of detrital background. Molybdenum would be expected to correlate with TOC, because adsorption of thiolated Mo to organic matter is the major pathway for Mo burial in sediments (Wilde et al., 2004; Helz et al., 2011). The absence of such a correlation in our data (**Figure 4C**) prohibits any inferences about Mo levels in the water column during the time of organic matter deposition. We can therefore not confirm previous suggestions for the presence of biogenic O_2 production during the time of deposition of these meta-sedimentary rocks (cf. Rosing and Frei, 2004).

It is, however, likely that these rocks have undergone some degree of hydrothermal alteration. Previous workers documented chalcopyrite in this geological unit (Rosing, 1999), and our good correlation between Cu and S (**Figure 4B**) is likely evidence for the presence of chalcopyrite. Copper [both Cu(I) and Cu(II)] is most soluble in saline and/or hot fluids, such as hydrothermal

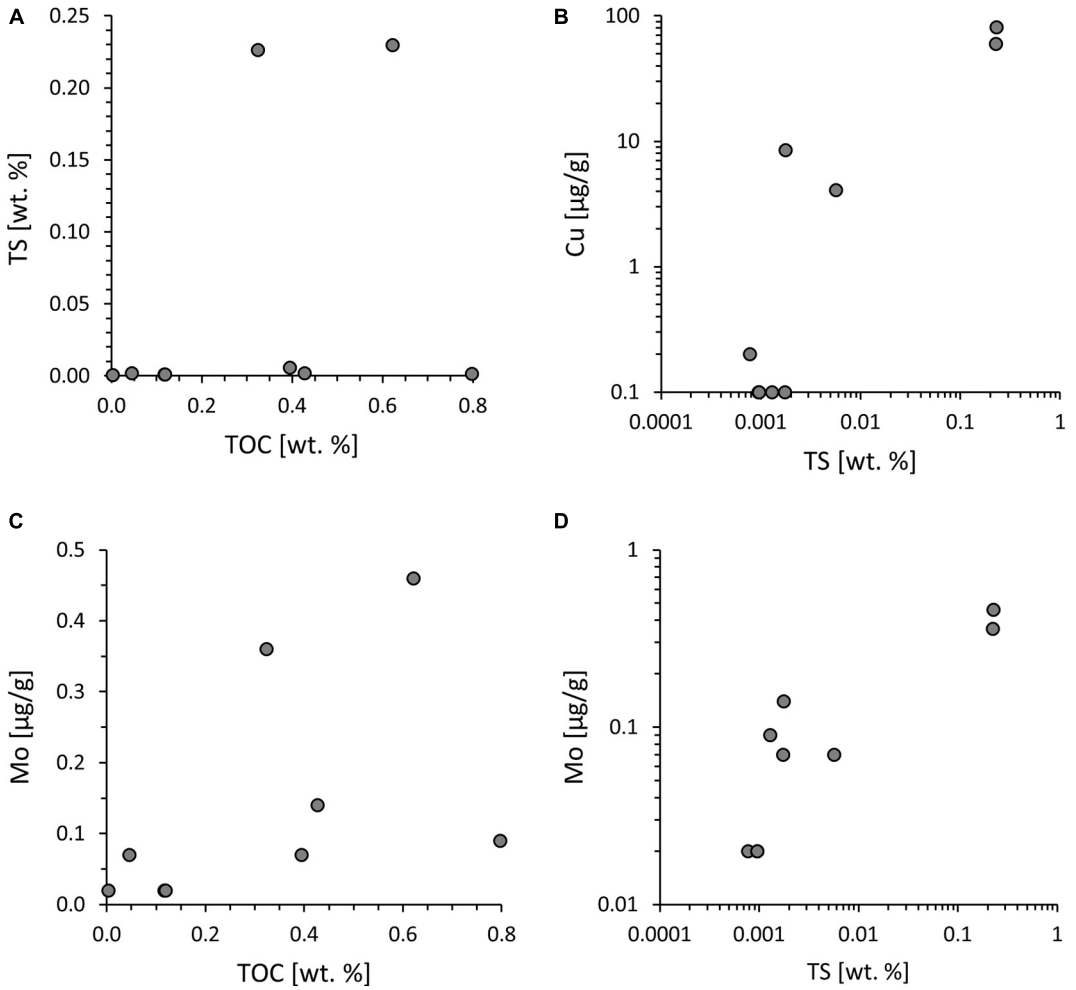

FIGURE 4 | Redox and hydrothermal alteration indicators. **(A)** Total sulfur (TS) vs. total organic carbon (TOC), showing no correlation. **(B)** Cu vs. TS. Given previous observations of chalcopyrite in these rocks (Rosing, 1999), the covariance between Cu and TS suggests a hydrothermal source of sulfur. **(C)** Mo vs. TOC, showing no correlation, counter to what is commonly observed in unaltered sedimentary rocks (Wilde et al., 2004). **(D)** Mo vs. TS, indicating that Mo may have been introduced by hydrothermal fluids along with Cu and sulfur.

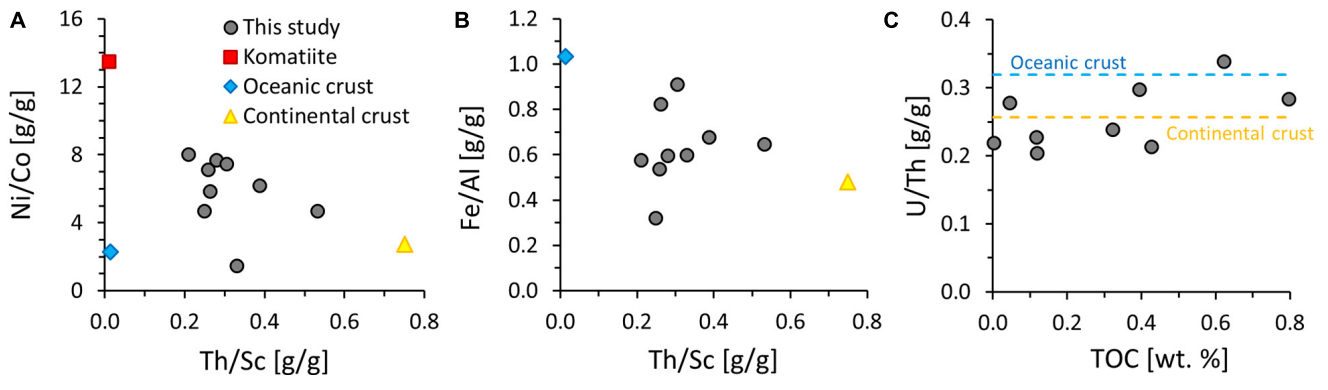

FIGURE 5 | Geochemical provenance and redox indicators. **(A)** Ni/Co vs. Th/Sc. **(B)** Fe/Al vs. Th/Sc. **(C)** U/Th vs. total organic carbon (TOC). Reference values for average crust and komatiite are taken from the literature (Rudnick and Gao, 2014; White and Klein, 2014; Ptáček et al., 2020).

effluents and relatively insoluble in cold seawater (Zhong et al., 2015). The Cu and S abundances in our samples are overall relatively low, and it is conceivable that Cu sulfides are detrital in origin. However, given the association of Cu with S, we cannot rule out minor hydrothermal overprinting. This conclusion is also consistent with our sulfur isotope data which plot close to the average upper mantle value of -1 ± 0.5 ‰ (Labidi et al., 2012) and may thus reflect contributions of hydrothermal H_2S derived from magmatic processes (Seal, 2006). Such hydrothermal fluids may have also introduced slightly elevated amounts of Mo into some of the samples, which also covaries with S (**Figure 4D**). Whether this hydrothermal activity was syn- or post-depositional cannot be resolved from our data, but its implications require consideration in the interpretation of the nitrogen isotope data.

Nitrogen Sources

In the form of ammonium (NH_4^+), nitrogen has the same charge and size as K^+ and Rb^+ and therefore partitions into similar mineral phases (Busigny and Bebout, 2013). This notion explains our dataset where the abundances for TN and K show a strong correlation ($R^2 = 0.89$; **Figure 3C**). It is thus conceivable that one major source of N are detrital mineral grains that were eroded from K-bearing igneous rocks (e.g., Hall, 1999). However, organic $\delta^{13}C$ values as well as previous hydrogen and nitrogen detections in the graphite in these rocks point toward the presence of biomass during the deposition of the turbidites (Rosing, 1999; Hassenkam et al., 2017). This graphitized biomass is thought to be derived from living organisms that were thriving on the seafloor or within the water column. When biomass gets buried in sediments and undergoes diagenesis, ammonium is released into porewaters, where it may accumulate to high concentrations in the mM range (e.g., Rosenfeld, 1979; Boudreau and Canfield, 1988). At such high concentrations, significant amounts of ammonium can substitute into K-bearing minerals, such as illite (Müller, 1977; Schroeder and McLain, 1998). This mechanism thus effectively transfers N from organic matter into silicate minerals and has even been invoked to explain elevated N abundances in granitoids (Hall, 1999). Hence if the graphite in our samples does indeed represent ancient biomass, then it is very likely that N was initially introduced in the form of organic molecules and later transferred to potassic minerals during diagenesis and/or metamorphism. The correlation between TN and K could therefore represent a diagenetic artifact rather than provenance.

However, we cannot rule out that the N-poor samples in our set contain significant contributions of detrital nitrogen. In fact, mixing between a detrital and authigenic component could well explain the correlation between TN and $\delta^{15}N$ that is difficult to explain by metamorphic effects alone. We can calculate this detrital endmember, if we make an assumption for its isotopic composition. As a first plausible guess, we assume that it has a composition of -5‰, i.e., similar to Earth's upper mantle and mafic crust (Cartigny and Marty, 2013). Two-endmember mixing of (i) detrital nitrogen with a composition of -5‰ and (ii) authigenic nitrogen with a composition of $+6.1$‰ (i.e., the mean value of the N-rich samples) would thus imply that the authigenic component of the three N-poor samples makes up between 61 and 72% while the rest is detrital; the detrital fraction would make up 1.6 ppm on average (range 1.4–1.7 ppm). It is likely that also the N-rich samples contain a similar detrital component, but if we correct the measured data under the assumption that 1.6 ppm of the total nitrogen is detrital in origin, the resulting $\delta^{15}N$ values increase only slightly from a mean of $+6.1$ to $+6.9$‰. Across all samples, the authigenic component would thus have a composition of $+6.7 \pm 0.8$‰ (**Figure 3A**). Hence detrital contributions are probably negligible for these relatively N-rich samples in our sample set (4–8% of total N).

Importantly, using a value of -5‰ for the detrital contribution, based on the composition of mantle-derived magmatic rocks (Cartigny and Marty, 2013), requires that this detrital component has not been affected by metamorphism in the same manner as the authigenic nitrogen in the same samples (see section "Metamorphic Effects on Nitrogen Geochemistry"). This assumption is plausible, because detrital minerals eroded from magmatic rocks have already been exposed to high temperatures and pressures and may therefore be resistant to metamorphism. Of course, magmatic rocks do undergo metamorphism as well, but magmatic N is likely fully lattice bound as the high temperatures under which the minerals formed would volatilize loosely bound material. Therefore, metamorphism of magmatic materials likely results in a smaller loss of N compared to materials in which N is predominantly organic-bound. Hence detrital magmatic minerals are expected to lose relatively less N during thermal metamorphism. However, if we take the more radical view that all three of the N-poor samples are 100% composed of detrital N with an average of 4.8 ppm and an isotopic value of $+2.3$‰ (i.e., allowing for metamorphic alteration and isotopic enrichment of detrital minerals), it would mean that the N-rich population contains between 76 and 87% authigenic N, and this authigenic N would have an isotopic value of $+7.0 \pm 0.8$‰. This result is very similar to the value of $+6.7 \pm 0.8$‰ calculated above, meaning that the uncertainty about the size and isotopic composition of the detrital component does not impact our overall conclusions. We will therefore proceed with the assumption that the authigenic N component in these samples falls around a mean $\delta^{15}N$ value of 6–7‰.

Metamorphic Effects on Nitrogen Geochemistry

The rocks investigated in this study have undergone metamorphic alteration up to mid-amphibolite facies (Rosing, 1999; Ramírez-Salazar et al., 2021), and it is well known that metamorphism strongly impacts N abundances and isotopic ratios in sedimentary rocks (Haendel et al., 1986; Bebout and Fogel, 1992; Boyd and Phillippot, 1998; Jia, 2006; Palya et al., 2011). The measured data do therefore not represent primary values. However, it is possible to quantify the degree of metamorphic alteration and to estimate the pre-metamorphic starting value, because the isotopic fractionation factors associated with partial N volatilization during metamorphism have been constrained in previous studies. For a temperature around 527°C, Hanschmann (1981) estimated $\alpha = 1.0073$ for N-loss as NH_3 (i.e., for the reaction NH_3–NH_4^+) and

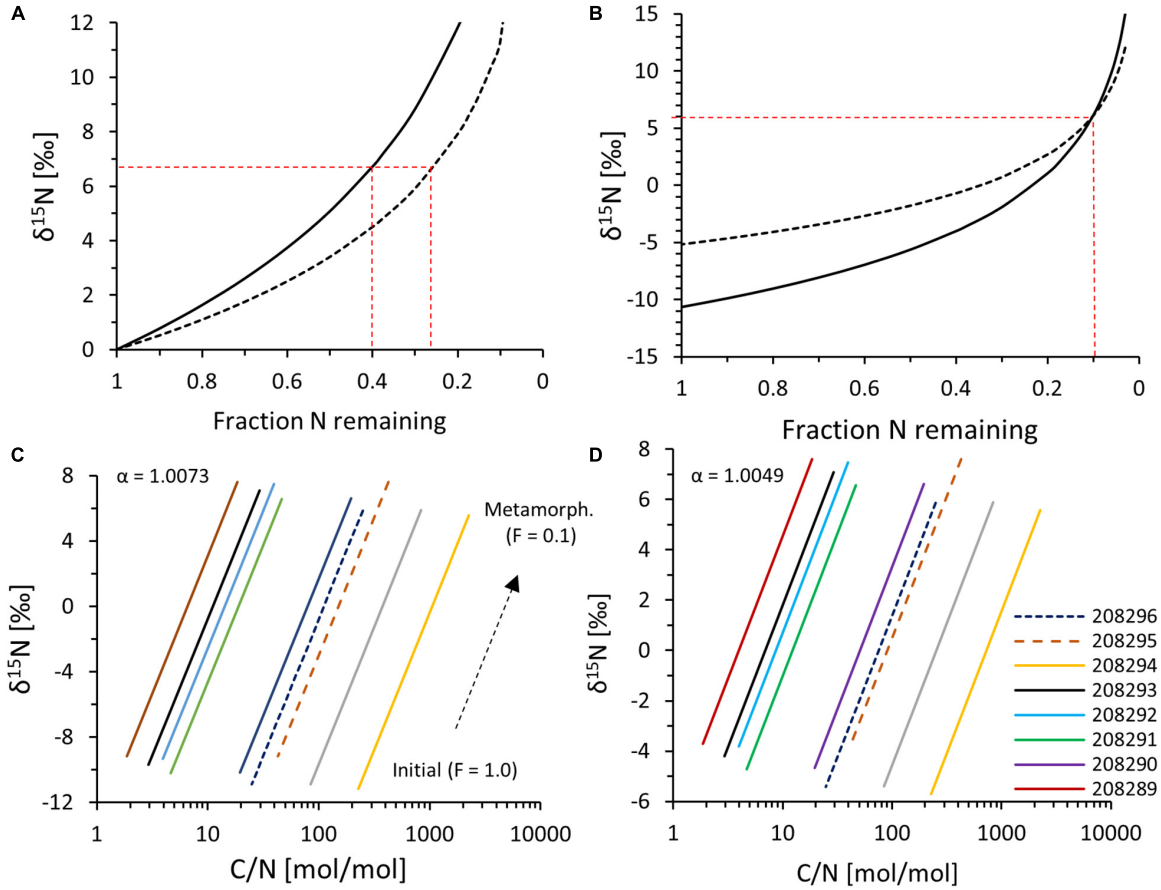

FIGURE 6 | (A) Rayleigh fractionation model with fixed $\delta^{15}N_{initial}$ = 0‰ and fractionation factors (α) of either 1.0049 (dashed line) or 1.0073 (solid line). Red dashed lines = F values corresponding to $\delta^{15}N$ = +6.7‰, which is the average authigenic N component. **(B)** Rayleigh fractionation model, adjusting $\delta^{15}N_{initial}$ such that $\delta^{15}N_{metamorphic}$ = +6.7‰ at F = 0.1. **(C)** Evolution of authigenic $\delta^{15}N$ and C/N ratios at α = 1.0073. **(D)** Evolution of authigenic $\delta^{15}N$ and C/N ratios at α = 1.0049.

α = 1.0049 for N-loss as N_2 (for the reaction N_2–NH_3), where $\alpha = (^{15}N/^{14}N)_{residue}/(^{15}N/^{14}N)_{volatile}$ (summarized by Haendel et al., 1986). These fractionation factors were found to be applicable to Archean rocks by Pinti et al. (2001). As the nitrogen speciation in our scenario is not known, we plot the maximum and minimum fractionation factors (**Figure 6**). We used a standard Rayleigh distillation equation $(\delta^{15}N_{metamorphic}/1000 + 1)/(\delta^{15}N_{initial}/1000 + 1) = F^{(1-\alpha)}$ where F = fraction nitrogen remaining, $\delta^{15}N_{initial}$ = initial $\delta^{15}N$ value, and $\delta^{15}N_{metamorphic}$ = metamorphic $\delta^{15}N$ value. Either F or $\delta^{15}N_{initial}$ can be calculated by assuming reasonable bounds for the respective other parameter.

At first, we fixed $\delta^{15}N_{initial}$ and calculated F. A plausible assumption for $\delta^{15}N_{initial}$ may be the composition of biological N_2-fixing organisms, which dominate $\delta^{15}N$ signals of younger Archean sedimentary rocks (Stüeken et al., 2016). We therefore set $\delta^{15}N_{initial}$ to 0‰ and calculated how much nitrogen would need to remain in the system (F) such that the calculated metamorphosed values ($\delta^{15}N_{metamorphic}$) match our observation (+6.7‰ for average authigenic N). The results suggest that about 24–40% (average 33%) of TN would have needed to be retained to shift authigenic $\delta^{15}N$ from 0 to +6.7‰ with a fractionation factor (α) of 1.0049–1.0073 (**Figure 6A**). However, such a high retention is inconsistent with previous studies that documented down to only 10% nitrogen retention at amphibolite facies (Haendel et al., 1986). The average TN retention found by Haendel et al. (1986) was 20%, while the maximum was around 10%. In a second calculation we therefore assumed that only 10% of TN has remained in the sample (i.e., F = 0.1) and varied $\delta^{15}N_{initial}$ until the isotopic composition of the residual measured nitrogen ($\delta^{15}N_{metamorphic}$) was equal to the calculated authigenic $\delta^{15}N$ value for each sample. The results point toward a starting composition of −4.6 ± 0.8‰ for α = 1.0049 and −10.1 ± 0.8‰ for α = 1.0073 with a mean of −7.3 ± 1.1‰ (**Figure 6B**). This value is close to the value of −7.1‰ that Pinti et al. (2001) reconstructed from a single sample of the same geological unit, using a stepwise combustion technique paired with argon isotope measurements. If we assume 20% N retention, our initial $\delta^{15}N$ values would fall between −1.2 and −5.2‰, which does not overlap with the value derived by Pinti et al. (2001). To further constrain TN retention, we looked at the reconstructed C/N ratios, which were calculated by changing

TN while holding TOC constant. In reality, some TOC is likely to have been lost as well during metamorphism, and so the reconstructed values represent an upper limit of the true initial C/N Redfield ratio. In the case of 10% retention, reconstructed C/N ratios fall around an average of 15 for the N-rich sample population, which is close to the Redfield ratio (C/N = 7–10) of microbial biomass (Godfrey and Glass, 2011; Algeo et al., 2014). For the case of 20% retention, the C/N ratios would be 30 on average and therefore further removed from the expected value of microbial biomass. This offset would be even larger if we account for loss of some TOC during metamorphism. A scenario with only 10% nitrogen retention, i.e., 90% TN loss during metamorphism, therefore appears more likely. In any case, the reconstructed C/N ratios vary widely between samples (range 2–226 for the 10% retention scenario, median 20, **Figures 6C,D**), but this variability may simply reflect diagenetic ammonium migration from organic-rich to organic-lean laminae, which is commonly observed in younger sedimentary successions (e.g., Koehler et al., 2019b). Overall, paired with the one data point collected by Pinti et al. (2001), our data suggest a starting $\delta^{15}N$ value that was significantly less ^{15}N-enriched than in younger Archean sedimentary rocks.

Pre-metamorphic Alteration

A pre-metamorphic $\delta^{15}N$ value around −1 to −10 ‰ in these Isua turbidites (Pinti et al., 2001, this study) may not necessarily represent the composition of biomass during the time of deposition. As noted above, we cannot rule out that these rocks have been exposed to at least mild hydrothermal alteration over their complex metamorphic history, as suggested by the presence of possibly hydrothermally-derived chalcopyrite. However, it is unlikely that post-depositional fluid circulation led to these light isotopic values by either subtraction or addition of nitrogen. First, experimental work has shown that the interaction between hot fluids and organic-bound N imparts minimal isotopic fractionation (<1‰) (Boudou et al., 2008). Hydrothermal leaching of N from these rocks is therefore unlikely to have induced such a large isotopic perturbation. Second, hydrothermal fluids are N-poor unless they circulate through sedimentary packages and mobilized ammonium from older organic matter (Lilley et al., 1993), for which there is no evidence in this field area. And even if older sedimentary rocks existed and provided a source of nitrogen to hydrothermal fluids, which was then added to our sample set, those older rocks would themselves have needed to contain isotopically light nitrogen. Hence there is no obvious mechanism by which hydrothermal fluids could have shifted initial $\delta^{15}N$ values downward by several permil.

Other studies of hydrothermally altered Precambrian rocks show strong isotopic perturbations, where organic-bound nitrogen has become isotopically depleted by up to 15‰ (Godfrey et al., 2013); however, in that case, the silicate-bound nitrogen fraction incorporated the complementary heavy nitrogen pool, such that the bulk rock value was within 2–3‰ of contemporaneous unaltered strata from the same basin. As we measured bulk rock values rather than kerogen isolates, this mechanism can therefore not explain our data. Therefore, we find no evidence for significant hydrothermal alteration of the ammonium contained in these samples, suggesting that the pre-metamorphic $\delta^{15}N$ value was between −1 and −10‰.

Eoarchean Biogeochemical Nitrogen Cycling

If primary $\delta^{15}N$ values were as high as −1‰, as inferred for 20% TN retention and a relatively small isotopic fractionation factor (section "Metamorphic Effects on Nitrogen Geochemistry"), this may be evidence for the presence of biological N_2 fixation as far back as 3.7 Ga. This interpretation would be consistent with phylogenetic data indicating an early evolution and ecological radiation of this metabolism, possibly dating back to the last universal common ancestor of life on Earth (Weiss et al., 2016; Parsons et al., 2020). However, if the lighter values are correct, which agree better with the previous estimate by Pinti et al. (2001) and are consistent with reconstructed C/N ratios, this may point toward a distinct geobiological N cycle at the time. First, such a low $\delta^{15}N$ value could reflect a different source of N to biological communities compared to later periods in Earth's history where $\delta^{15}N$ rarely drops below −2‰ (Stüeken et al., 2016). One possible explanation may be biological N_2 fixation with a so-called alternative nitrogenase. These enzymes contain either V or Fe instead of Mo in their catalytic center and impart isotopic fractionation down to −8 ‰ during the conversion of N_2 to NH_4^+ (Zhang et al., 2014). They are rarely expressed in natural environments today, but Mo scarcity in the early Archean ocean may potentially have favored V- or Fe-based nitrogenase (Raymond et al., 2004; Scott et al., 2008). However, the scarcity of similarly light $\delta^{15}N$ values throughout the rest of the Archean then becomes puzzling. Furthermore, phylogenetic data suggest that V- and Fe-based nitrogenases may not have radiated until the late Proterozoic (Parsons et al., 2020), making it unlikely that they were important players in the Eoarchean N cycle. Alternatively, isotopically light N may have been derived from atmospheric rainout of lightning products or HCN. HCN can form during photolysis in the upper atmosphere (Tian et al., 2011), and experimental data revealed an isotopic composition of −15 to −25‰ (Kuga et al., 2014). The composition of lightning products such as NOx is so far poorly constrained, but some existing measurements from the modern atmosphere show light values around −5 to −15‰ (Moore, 1977). Atmospheric N-bearing molecules could thus be a plausible explanation for our results. Phylogenetic data are consistent with early utilization of NOx species, possibly derived from lightning (Parsons et al., 2020). If so, it would imply that the atmospheric nitrogen source declined in relative importance between the Eoarchean and younger Archean (3.2 Ga onward) where such light values are no longer observed and N metabolisms are dominated by anaerobic pathways (Parsons et al., 2020). A third possible explanation for light $\delta^{15}N$ in biomass is partial assimilation of ammonium from a large, dissolved ammonium pool in seawater. Culturing experiments with modern microorganisms show fractionation factors of

−4 to −27‰ if ammonium concentrations exceed ca. 10–20 μM (Hoch et al., 1992). However, given the high metabolic costs of converting N_2 into ammonium and the inefficiency of abiotic ammonium accumulation in seawater (Stüeken, 2016), it is unlikely that such a large ammonium pool existed. In summary, the meaning of these light values in Eoarchean rocks, if correct, remains elusive, but atmospheric rainout of isotopically light bioavailable N species is at present perhaps the most plausible explanation.

Nitrogen Recycling Into Earth's Mantle?

If our reconstruction is correct, and if these values are representative of the Eoarchean (which we cannot confirm from a single outcrop), then this may have implications for the secular evolution of key geological N reservoirs over Earth's history. Today Earth's lower mantle, upper mantle and surface reservoirs show striking and intriguing isotopic imbalances. The upper mantle shows an average $\delta^{15}N$ value of ca. -5 ± 3‰, as determined by measurements of diamonds, kimberlite xenoliths and mid-ocean ridge basalt (Cartigny and Marty, 2013). This negative upper mantle value is thought to date back to the Archean as indicated by diamonds from 3.3 to 2.9 Ga which display a mode around -5 ± 3‰ (Richardson et al., 2001; Cartigny, 2005). In contrast, plume sources for ocean island basalts—assumed to originate from lower mantle domains below the upper mantle—are weakly positive in $\delta^{15}N$, similar to post-Archean crustal reservoirs (Marty and Dauphas, 2003). Since the Great Oxidation Event in the Paleoproterozoic (∼2.5 Ga), crustal materials are dominantly enriched in ^{15}N (>+2‰) (Zerkle et al., 2017; Kipp et al., 2018), and most of the Archean sedimentary record between 3.2 and 2.5 Ga falls around values of 0‰ (Stüeken et al., 2015; Homann et al., 2018; Koehler et al., 2019a; Ossa Ossa et al., 2019). Isotopically lighter values are rare in open marine settings and mostly restricted to organic extracts, which are distinct from bulk rock values (Beaumont and Robert, 1999; Yang et al., 2019). Hence Earth's upper mantle and exterior (crust + atmosphere) appear to have displayed an isotopic imbalance for the last 3.2 billion years (Boyd and Pillinger, 1994). This is intriguing, because degassing of the upper mantle and/or the subduction of sedimentary nitrogen should generate a more ^{15}N-enritched upper mantle (Boyd and Pillinger, 1994).

However, if the positive $\delta^{15}N$ values in plumes from the lower mantle are primary and reflect the initial mantle $\delta^{15}N$ value, then one possible explanation for the isotopic imbalance of the upper mantle is the subduction of isotopically light sedimentary rocks in the Eoarchean This hypothesis is not new (Marty and Dauphas, 2003; Cartigny, 2005; Cartigny and Marty, 2013), but has perhaps lost momentum because several recent studies of Mesoarchean rocks revealed sedimentary $\delta^{15}N$ values 0‰ (Stüeken et al., 2015; Homann et al., 2018; Koehler et al., 2019a; Ossa Ossa et al., 2019). However, our new findings open up the possibility that the Eoarchean N cycle may have been distinct, in particular if it involved a stronger involvement of atmospheric products that were incorporated into ancient biomass. It is therefore conceivable that during the first one billion years of Earth's history nitrogen in sediments was more akin to the modern upper mantle $\delta^{15}N$ value. If correct, this may fuel the idea that the mantle inherited its light value from Eoarchean sediment recycling. We stress that a geodynamic mechanism for such a model is so far ambiguous, and it remains to be determined if the total volume of isotopically light sedimentary rocks would have been large enough to change the isotopic value of the mantle. For example, the subduction of sedimentary N with negative $\delta^{15}N$ values would only control the upper mantle $\delta^{15}N$ value if the mass of subducted sedimentary N is far greater than the N abundance of the upper mantle to account for loss by degassing. The abundance and distribution of nitrogen throughout the deep silicate Earth is a topic of much debate (Zerkle and Mikhail, 2017), but our results suggest that this may be a worthwhile avenue to pursue in future studies.

CONCLUSION

Reconstructing the conditions under which life emerged and thrived on the early Earth is pivotal for delineating constraints on the habitability of other worlds. The poor preservation of the oldest sedimentary rock record presents a clear impediment to this line of research; however, our results add to a growing body of literature showing that some information can be extracted if metamorphic effects are appropriately accounted for. In this case, we find that amphibolite-grade meta-sedimentary rocks from the Isua Supracrustal Belt contain several μg N per g of bulk rock with an average $\delta^{15}N$ value of +6.1‰, and most of this nitrogen appears to be bound in potassic phases. However, knowledge of the diagenetic and metamorphic behavior of nitrogen allows us to reconstruct that the initial nitrogen endowment of these rocks was likely derived from buried biomass, and this biogenic nitrogen appears to have been isotopically depleted with $\delta^{15}N$ values down to −1 to −10‰ and most likely below −5‰. This result is consistent with previous work that estimated a value of −7‰ (Pinti et al., 2001). Hydrothermal alteration cannot easily be evoked to explain such a light initial value. Instead, we speculate that the Eoarchean nitrogen cycle was strongly influenced by atmospheric rainout of NOx species and/or HCN, which could explain these light $\delta^{15}N$ values (Moore, 1977; Kuga et al., 2014). This conclusion supports the idea that recycling of Eoarchean sedimentary rocks may have created the isotopic dichotomy between Earth's exterior and interior that appears to have existed since at least 3.2 Ga (Richardson et al., 2001; Cartigny, 2005; Cartigny and Marty, 2013), although we stress that a geodynamic model in support of this view requires significant developmental work (beyond the scope of this study).

Importantly, the imprint of isotopically light atmospheric products is absent from the younger Archean record (Ader et al., 2016; Stüeken et al., 2016). From the Mesoarchean onward Earth's biosphere appears to have been fueled by biological Mo-based nitrogenase-driven N_2 fixation (Parsons et al., 2020). We speculate that the transition from mostly abiotic N sources to biological N_2 fixation reflects an increase in biological productivity, which "encouraged" the invention and expansion of N_2-fixing enzymes. If so, then atmospheric processes may have been important for origin of life, but they were perhaps not sufficient for sustaining a large biosphere over geologic timescales.

DATA AVAILABILITY STATEMENT

The original contributions presented in the study are included in the article/supplementary material, further inquiries can be directed to the corresponding author/s.

AUTHOR CONTRIBUTIONS

KS collected the samples. NG established the connections between researchers. ES and TB analyzed the samples. SM contributed to the interpretation of the data. ES wrote the manuscript with inputs from all authors. All authors contributed to the article and approved the submitted version.

FUNDING

ES acknowledges support from the School of Earth and Environmental Sciences at St Andrews. TB was funded by a NERC IAPETUS Doctoral Training Program (NE/R012253/1) studentship. Fieldwork at Isua was supported by the Carlsberg Foundation through grant CF18-0090 to KS.

REFERENCES

Ader, M., Thomazo, C., Sansjofre, P., Busigny, V., Papineau, D., Laffont, R., et al. (2016). Interpretation of the nitrogen isotopic composition of precambrian sedimentary rocks: assumptions and perspectives. *Chem. Geol.* 429, 93–110. doi: 10.1016/j.chemgeo.2016.02.010

Algeo, T. J., Meyers, P. A., Robinson, R. S., Rowe, H., and Jiang, G. Q. (2014). Icehouse-greenhouse variations in marine denitrification. *Biogeosciences* 11, 1273–1295. doi: 10.5194/bg-11-1273-2014

Baadsgaard, H., Nutman, A. P., Bridgwater, D., Rosing, M., McGregor, V. R., and Allaart, J. H. (1984). The zircon geochronology of the akilia association and Isua supracrustal belt, West Greenland. *Earth Planetary Sci. Lett.* 68, 221–228. doi: 10.1016/0012-821x(84)90154-7

Barry, P. H., and Hilton, D. R. (2016). Release of subducted sedimentary nitrogen throughout Earth's mantle. *Geochem. Perspect. Lett.* 2, 148–159. doi: 10.7185/geochemlet.1615

Beaumont, V., and Robert, F. (1999). Nitrogen isotope ratios of kerogens in Precambrian cherts: a record of the evolution of atmosphere chemistry? *Precambrian Res.* 96, 63–82. doi: 10.1016/s0301-9268(99)00005-4

Bebout, G. E., and Fogel, M. L. (1992). Nitrogen-isotopic composition of metasedimentary rocks in the Catalina Schist, California: implications for metamorphic devolatilization history. *Geochimica et Cosmochimica Acta* 56, 2839–2849. doi: 10.1016/0016-7037(92)90363-n

Boak, J. L., and Dymek, R. F. (1982). Metamorphism of the ca. 3800 Ma supracrustal rocks at Isua, West Greenland: implications for early Archaean crustal evolution. *Earth Planetary Sci. Lett.* 59, 155–176. doi: 10.1016/0012-821x(82)90123-6

Boocock, T. J., Mikhail, S., Prytulak, J., Di Rocco, T., and Stüeken, E. E. (2020). Nitrogen mass fraction and stable isotope ratios for fourteen geological reference materials: evaluating the applicability of elemental analyser versus sealed tube combustion methods. *Geostand. Geoanal. Res.* 44, 537–551. doi: 10.1111/ggr.12345

Boudou, J. P., Schimmelmann, A., Ader, M., Mastalerz, M., Sebilo, M., and Gengembre, L. (2008). Organic nitrogen chemistry during low-grade metamorphism. *Geochimica et Cosmochimica Acta* 72, 1199–1221. doi: 10.1016/j.gca.2007.12.004

Boudreau, B. P., and Canfield, D. E. (1988). A provisional diagenetic model for pH in anoxic porewaters: application to the FOAM site. *J. Mar. Res.* 46, 429–455. doi: 10.1357/002224088785113603

Boyd, S. R., and Phillippot, P. (1998). Precambrian ammonium biogeochemistry: a study of the moine metasediments, Scotland. *Chem. Geol.* 144, 257–268. doi: 10.1016/s0009-2541(97)00135-6

Boyd, S. R., and Pillinger, C. T. (1994). A preliminary study of 15N/14N in octahedral growth form diamonds. *Chem. Geol.* 116, 43–59. doi: 10.1016/0009-2541(94)90157-0

Busigny, V., and Bebout, G. E. (2013). Nitrogen in the silicate earth: speciation and isotopic behavior during mineral–fluid interactions. *Elements* 9, 353–358. doi: 10.2113/gselements.9.5.353

Busigny, V., Cartigny, P., Laverne, C., Teagle, D., Bonifacie, M., and Agrinier, P. (2019). A re-assessment of the nitrogen geochemical behavior in upper oceanic crust from Hole 504B: implications for subduction budget in Central America. *Earth Planetary Sci. Lett.* 525:115735. doi: 10.1016/j.epsl.2019.115735

Cartigny, P. (2005). Stable isotopes and the origin of diamond. *Elements* 1, 79–84. doi: 10.2113/gselements.1.2.79

Cartigny, P., and Marty, B. (2013). Nitrogen isotopes and mantle geodynamics: the emergence of life and the atmosphere–crust–mantle connection. *Elements* 9, 359–366. doi: 10.2113/gselements.9.5.359

Feng, L., Li, H., and Liu, W. (2018). Nitrogen Mass fraction and isotope determinations in geological reference materials using sealed-tube combustion coupled with continuous-flow isotope-ratio mass spectrometry. *Geostand. Geoanal. Res.* 42, 539–548. doi: 10.1111/ggr.12234

Friend, C. R., and Nutman, A. P. (2019). Tectono-stratigraphic terranes in Archaean gneiss complexes as evidence for plate tectonics: the Nuuk region, southern West Greenland. *Gondwana Res.* 72, 213–237. doi: 10.1016/j.gr.2019.03.004

Godfrey, L. V., and Glass, J. B. (2011). The geochemical record of the ancient nitrogen cycle, nitrogen isotopes, and metal cofactors. *Methods Enzymol.* 486, 483–506. doi: 10.1016/b978-0-12-381294-0.00022-5

Godfrey, L. V., Poulton, S. W., Bebout, G. E., and Fralick, P. W. (2013). Stability of the nitrogen cycle during development of sulfidic water in the redox-stratified late Paleoproterozoic ocean. *Geology* 41, 655–658.

Guotana. (submitted). Deserpentinization and high pressure (eclogite-facies) metamorphic features in the Eoarchean ultramafic body from Isua, Greenland. *Geosci. Front.*

Haendel, D., Muehle, K., Nitzsche, H.-M., Stiehl, G., and Wand, U. (1986). Isotopic variations of the fixed nitrogen in metamorphic rocks. *Geochimica et Cosmochimica Acta* 50, 749–758.

Hall, A. (1999). Ammonium in granites and its petrogenetic significance. *Earth Sci. Rev.* 45, 145–165.

Hanmer, S., and Greene, D. C. (2002). A modern structural regime in the Paleoarchean (3.64 Ga); Isua greenstone belt, southern West Greenland. *Tectonophysics* 346, 201–222. doi: 10.1016/s0040-1951(02)00029-x

Hanschmann, G. (1981). Berechnung von Isotopieeffekten auf quantenchemischer Grundlage am beispiel stickstoffhaltiger molecule. *Zfl-Mitteilungen* 41, 19–39.

Hassenkam, T., Andersson, M. P., Dalby, K. N., Mackenzie, D. M. A., and Rosing, M. T. (2017). Elements of eoarchean life trapped in mineral inclusions. *Nature* 548, 78–81. doi: 10.1038/nature23261

Helz, G. R., Bura-Nakic, E., Mikac, N., and Ciglenecki, I. (2011). New model for molybdenum behavior in euxinic waters. *Chem. Geol.* 284, 323–332. doi: 10.1016/j.chemgeo.2011.03.012

Hoch, M. P., Fogel, M. L., and Kirchman, D. L. (1992). Isotope fractionation associated with ammonium uptake by a marine bacterium. *Limnol. Oceanogr.* 37, 1447–1459. doi: 10.4319/lo.1992.37.7.1447

Hoffmann, J. E., Münker, C., Polat, A., König, S., Mezger, K., and Rosing, M. T. (2010). Highly depleted Hadean mantle reservoirs in the sources of early Archean arc-like rocks, Isua supracrustal belt, southern West Greenland. *Geochimica et Cosmochimica Acta* 74, 7236–7260. doi: 10.1016/j.gca.2010.09.027

Homann, M., Sansjofre, P., Van Zuilen, M., Heubeck, C., Gong, J., Killingsworth, B., et al. (2018). Microbial life and biogeochemical cycling on land 3,220 million years ago. *Nat. Geosci.* 11, 665–671. doi: 10.1038/s41561-018-0190-9

Jenner, F. E., Bennett, V. C., Nutman, A. P., Friend, C. R. L., Norman, M. D., and Yaxley, G. (2009). Evidence for subduction at 3.8 Ga: geochemistry of arc-like

metabasalts from the southern edge of the Isua Supracrustal Belt. *Chem. Geol.* 261, 83–98. doi: 10.1016/j.chemgeo.2008.09.016

Jia, Y. (2006). Nitrogen isotope fractionations during progressive metamorphism: a case study from the Paleozoic Cooma metasedimentary complex, southeastern Australia. *Geochimica et Cosmochimica Acta* 70, 5201–5214. doi: 10.1016/j.gca.2006.08.004

Kamber, B. S., Whitehouse, M. J., Bolhar, R., and Moorbath, S. (2005). Volcanic resurfacing and the early terrestrial crust: zircon U–Pb and REE constraints from the Isua Greenstone Belt, southern West Greenland. *Earth Planetary Sci. Lett.* 240, 275–290.

Kipp, M. A., Stüeken, E. E., Yun, M., Bekker, A., and Buick, R. (2018). Pervasive aerobic nitrogen cycling in the surface ocean across the Paleoproterozoic Era. *Earth Planetary Sci. Lett.* 500, 117–126. doi: 10.1016/j.epsl.2018.08.007

Koehler, M. C., Buick, R., and Barley, M. E. (2019a). Nitrogen isotope evidence for anoxic deep marine environments from the mesoarchean mosquito creek formation, Australia. *Precambrian Res.* 320, 281–290. doi: 10.1016/j.precamres.2018.11.008

Koehler, M. C., Stüeken, E. E., Hillier, S., and Prave, A. R. (2019b). Limitation of fixed nitrogen and deepening of the carbonate-compensation depth through the Hirnantian at Dob's Linn, Scotland. *Palaeogeogr. Palaeoclimatol. Palaeoecol.* 534:109321. doi: 10.1016/j.palaeo.2019.109321

Kuga, M., Carrasco, N., Marty, B., Marrocchi, Y., Bernard, S., Rigaudier, T., et al. (2014). Nitrogen isotopic fractionation during abiotic synthesis of organic solid particles. *Earth Planetary Sci. Lett.* 393, 2–13. doi: 10.1016/j.epsl.2014.02.037

Labidi, J., Cartigny, P., Birck, J. L., Assayag, N., and Bourrand, J. J. (2012). Determination of multiple sulfur isotopes in glasses: a reappraisal of the MORB δ34S. *Chem. Geol.* 334, 189–198. doi: 10.1016/j.chemgeo.2012.10.028

Lepot, K. (2020). Signatures of early microbial life from the Archean (4 to 2.5 Ga) eon. *Earth Sci. Rev.* 209:103296. doi: 10.1016/j.earscirev.2020.103296

Lilley, M. D., Butterfield, D. A., Olson, E. J., Lupton, J. E., Macko, S. A., and McDuff, R. E. (1993). Anomalous CH4 and NH4+ concentrations at an unsedimented mid-ocean-ridge hydrothermal system. *Nature* 364, 45–47. doi: 10.1038/364045a0

Lyons, T. W., and Severmann, S. (2006). A critical look at iron paleoredox proxies: new insights from modern euxinic marine basins. *Geochimica et Cosmochimica Acta* 70, 5698–5722. doi: 10.1016/j.gca.2006.08.021

Marty, B., and Dauphas, N. (2003). The nitrogen record of crust-mantle interaction and mantle convection from Archean to present. *Earth Planetary Sci. Lett.* 206, 397–410. doi: 10.1016/s0012-821x(02)01108-1

Mikhail, S., and Sverjensky, D. A. (2014). Nitrogen speciation in upper mantle fluids and the origin of Earth's nitrogen-rich atmosphere. *Nat. Geosci.* 7, 816–819. doi: 10.1038/ngeo2271

Moorbath, S., O'nions, R. K., and Pankhurst, R. J. (1973). Early archaean age for the isua iron formation, west greenland. *Nature* 245, 138–139. doi: 10.1038/245138a0

Moorbath, S., O'nions, R. K., and Pankhurst, R. J. (1975). The evolution of early Precambrian crustal rocks at Isua, West Greenland—geochemical and isotopic evidence. *Earth Planetary Sci. Lett.* 27, 229–239. doi: 10.1016/0012-821x(75)90034-5

Moore, H. (1977). The isotopic composition of ammonia, nitrogen dioxide and nitrate in the atmosphere. *Atmos. Environ.* 11, 1239–1243. doi: 10.1016/0004-6981(77)90102-0

Müller, P. J. (1977). CN ratios in Pacific deep-sea sediments: effect of inorganic ammonium and organic nitrogen compounds sorbed by clays. *Geochimica et Cosmochimica Acta* 41, 765–776. doi: 10.1016/0016-7037(77)90047-3

Myers, J. S. (2001). Protoliths of the 3.8–3.7 Ga Isua greenstone belt, west Greenland. *Precambrian Res.* 105, 129–141. doi: 10.1016/s0301-9268(00)00108-x

Nutman, A. P., Allaart, J. H., Bridgwater, D., Dimroth, E., and Rosing, M. (1984). Stratigraphic and geochemical evidence for the depositional environment of the early Archaean Isua supracrustal belt, southern West Greenland. *Precambrian Res.* 25, 365–396. doi: 10.1016/0301-9268(84)90010-x

Nutman, A. P., and Friend, C. R. (2009). New 1: 20,000 scale geological maps, synthesis and history of investigation of the Isua supracrustal belt and adjacent orthogneisses, southern West Greenland: a glimpse of Eoarchaean crust formation and orogeny. *Precambrian Res.* 172, 189–211. doi: 10.1016/j.precamres.2009.03.017

Nutman, A. P., Bennett, V. C., Friend, C. R., and Van Kranendonk, M. (2019). The Eoarchean legacy of Isua (Greenland) worth preserving for future generations. *Earth Sci. Rev.* 198:102923. doi: 10.1016/j.earscirev.2019.102923

Nutman, A. P., Bennett, V. C., Friend, C. R., and Yi, K. (2020). Eoarchean contrasting ultra-high-pressure to low-pressure metamorphisms (<250 to >1000°C/GPa) explained by tectonic plate convergence in deep time. *Precambrian Res.* 344:105770. doi: 10.1016/j.precamres.2020.105770

Nutman, A. P., McGregor, V. R., Friend, C. R., Bennett, V. C., and Kinny, P. D. (1996). The Itsaq gneiss complex of southern West Greenland; the world's most extensive record of early crustal evolution (3900-3600 Ma). *Precambrian Res.* 78, 1–39. doi: 10.1016/j.gca.2020.03.043

Ossa Ossa, F., Hofmann, A., Spangenberg, J. E., Poulton, S. W., Stüeken, E. E., Schoenberg, R., et al. (2019). Limited oxygen production in the Mesoarchean ocean. *Proc. Natl. Acad. Sci. U.S.A.* 116, 6647–6652. doi: 10.1073/pnas.1818762116

Palya, A. P., Buick, I. S., and Bebout, G. E. (2011). Storage and mobility of nitrogen in the continental crust: evidence from partially melted metasedimentary rocks, Mt. Stafford, Australia. *Chem. Geol.* 281, 211–226. doi: 10.1016/j.chemgeo.2010.12.009

Parsons, C., Stüeken, E. E., Rosen, C., Mateos, K., and Anderson, R. (2020). Radiation of nitrogen-metabolizing enzymes across the tree of life tracks environmental transitions in Earth history. *Geobiology* 19, 18–34. doi: 10.1111/gbi.12419

Pinti, D. L., Hashizume, K., and Matsuda, J. I. (2001). Nitrogen and argon signatures in 3.8 to 2.8 Ga metasediments: clues on the chemical state of the Archean ocean and the deep biosphere. *Geochimica et Cosmochimica Acta* 65, 2301–2315. doi: 10.1016/s0016-7037(01)00590-7

Polat, A., Hofmann, A. W., and Rosing, M. T. (2002). Boninite-like volcanic rocks in the 3.7–3.8 Ga Isua greenstone belt, West Greenland: geochemical evidence for intra-oceanic subduction zone processes in the early Earth. *Chem. Geol.* 184, 231–254. doi: 10.1016/s0009-2541(01)00363-1

Ptáček, M. P., Dauphas, N., and Greber, N. D. (2020). Chemical evolution of the continental crust from a data-driven inversion of terrigenous sediment compositions. *Earth Planetary Sci. Lett.* 539:116090. doi: 10.1016/j.epsl.2020.116090

Raiswell, R., Hardisty, D. S., Lyons, T. W., Canfield, D. E., Owens, J., Planavsky, N., et al. (2019). The iron paleoredox proxies: a guide to the pitfalls, problems and proper practice. *Am. J. Sci.* 318, 491–526. doi: 10.2475/05.2018.03

Ramírez-Salazar, A., Müller, T., Piazolo, S., Webb, A. A. G., Hauzenberger, C., Zuo, J., et al. (2021). Tectonics of the Isua supracrustal belt 1: P-T-X-d constraints of a poly-metamorphic terrane. *Tectonics* 40:e2020TC006516.

Raymond, J., Siefert, J. L., Staples, C. R., and Blankenship, R. E. (2004). The natural history of nitrogen fixation. *Mol. Biol. Evol.* 21, 541–554.

Richardson, S. H., Shirey, S. B., Harris, J. W., and Carlson, R. W. (2001). Archean subduction recorded by Re–Os isotopes in eclogitic sulfide inclusions in kimberley diamonds. *Earth Planetary Sci. Lett.* 191, 257–266. doi: 10.1016/s0012-821x(01)00419-8

Rollinson, H. (2002). The metamorphic history of the Isua greenstone belt, West Greenland. *Geol. Soc. Lond. Special Publications* 199, 329–350. doi: 10.1144/gsl.sp.2002.199.01.16

Rollinson, H. (2003). Metamorphic history suggested by garnet-growth chronologies in the Isua Greenstone Belt, West Greenland. *Precambrian Res.* 126, 181–196. doi: 10.1016/s0301-9268(03)00094-9

Rosenfeld, J. K. (1979). Ammonium adsorption in nearshore anoxic sediments. *Limnol. Oceanogr.* 24, 356–364. doi: 10.4319/lo.1979.24.2.0356

Rosing, M. T. (1999). 13C-depleted carbon microparticles in > 3700-Ma sea-floor sedimentary rocks from West Greenland. *Science* 283, 674–676. doi: 10.1126/science.283.5402.674

Rosing, M. T., and Frei, R. (2004). U-rich Archaean sea-floor sediments from Greenland–indications of >3700 Ma oxygenic photosynthesis. *Earth Planetary Sci. Lett.* 217, 237–244. doi: 10.1016/s0012-821x(03)00609-5

Rosing, M. T., Rose, N. M., Bridgwater, D., and Thomsen, H. S. (1996). Earliest part of Earth's stratigraphic record: a reappraisal of the> 3.7 Ga Isua (Greenland) supracrustal sequence. *Geology* 24, 43–46. doi: 10.1130/0091-7613(1996)024<0043:epoess>2.3.co;2

Rudnick, R. L., and Gao, S. (2014). Composition of the continental crust. *Treatise Geochem.* 4, 1–51. doi: 10.1016/b0-08-043751-6/03016-4

Schidlowski, M. (2001). Carbon isotopes as biogeochemical recorders of life over 3.8 Ga of earth history: evolution of a concept. *Precambrian Res.* 106, 117–134. doi: 10.1016/s0301-9268(00)00128-5

Schroeder, P. A., and McLain, A. A. (1998). Illite-smectites and the influence of burial diagenesis on the geochemical cycling of nitrogen. *Clay Miner.* 33, 539–546. doi: 10.1180/000985598545877

Scott, C., Lyons, T. W., Bekker, A., Shen, Y., Poulton, S. W., Chu, X., et al. (2008). Tracing the stepwise oxygenation of the Proterozoic ocean. *Nature* 452, 456–459. doi: 10.1038/nature06811

Seal, R. R. (2006). Sulfur isotope geochemistry of sulfide minerals. *Rev. Mineral. Geochem.* 61, 633–677. doi: 10.1515/9781501509490-013

Stüeken, E. E. (2016). Nitrogen in ancient mud: a biosignature? *Astrobiology* 16, 730–735. doi: 10.1089/ast.2016.1478

Stüeken, E. E., Boocock, T. J., Robinson, A., Mikhail, S., and Johnson, B. W. (2021). Hydrothermal recycling of sedimentary ammonium into oceanic crust and the Archean ocean at 3.24 Ga. *Geoloy* 49. doi: 10.1130/G48844.1

Stüeken, E. E., Buick, R., Anderson, R. E., Baross, J. A., Planavsky, N., and Lyons, T. W. (2017). Environmental niches and biodiversity in Neoarchean lakes. *Geobiology* 15, 767–783. doi: 10.1111/gbi.12251

Stüeken, E. E., Buick, R., Guy, B. M., and Koehler, M. C. (2015). Isotopic evidence for biological nitrogen fixation by Mo-nitrogenase at 3.2 Gyr. *Nature* 520, 666–669. doi: 10.1038/nature14180

Stüeken, E. E., Jones, S., Raub, T. D., Prave, A. R., Rose, C. V., Linnekogel, S., et al. (2020). Geochemical fingerprints of seawater in the Late Mesoproterozoic Midcontinent Rift, North America: life at the marine-land divide. *Chem. Geol.* 553:119812. doi: 10.1016/j.chemgeo.2020.119812

Stüeken, E. E., Kipp, M. A., Koehler, M. C., and Buick, R. (2016). The evolution of earth's biogeochemical nitrogen cycle. *Earth Sci. Rev.* 160, 220–239. doi: 10.1016/j.earscirev.2016.07.007

Thomazo, C., and Papineau, D. (2013). Biogeochemical cycling of nitrogen on the early earth. *Elements* 9, 345–351. doi: 10.2113/gselements.9.5.345

Tian, F., Kasting, J. F., and Zahnle, K. (2011). Revisiting HCN formation in Earth's early atmosphere. *Earth Planetary Sci. Lett.* 308, 417–423. doi: 10.1016/j.epsl.2011.06.011

Tribovillard, N., Algeo, T. J., Lyons, J., and Riboulleau, A. (2006). Trace metals as paleoredox and paleoproductivity proxies: an update. *Chem. Geol.* 232, 12–32.

Waterton, (submitted). A cumulate origin for Isua dunites rules out formation as an Eoarchaean ophiolite. *Geology*.

Webb, A. A. G., Müller, T., Zuo, J., Haproff, P. J., and Ramírez-Salazar, A. (2020). A non–plate tectonic model for the Eoarchean Isua supracrustal belt. *Lithosphere* 12, 166–179.

Weiss, M. C., Sousa, F. L., Mrnjavac, N., Neukirchen, S., Roettger, M., Nelson-Sathi, S., et al. (2016). The physiology and habitat of the last universal common ancestor. *Nat. Microbiol.* 1:16116.

White, W. M., and Klein, E. M. (2014). Composition of the oceanic crust. *Treatise Geochem.* 4, 457–496. doi: 10.1016/b978-0-08-095975-7.00315-6

Whitehouse, M. J., Myers, J. S., and Fedo, C. M. (2009). The akilia controversy: field, structural and geochronological evidence questions interpretations of> 3.8 Ga life in SW Greenland. *J. Geol. Soc.* 166, 335–348. doi: 10.1144/0016-76492008-070

Wilde, P., Lyons, T. W., and Quinby-Hunt, M. S. (2004). Organic carbon proxies in black shales: molybdenum. *Chem. Geol.* 206, 167–176. doi: 10.1016/j.chemgeo.2003.12.005

Yang, J., Junium, C. K., Grassineau, N. V., Nisbet, E. G., Izon, G., Mettam, C., et al. (2019). Ammonium availability in the Late Archaean nitrogen cycle. *Nat. Geosci.* 12, 553–557. doi: 10.1038/s41561-019-0371-1

Zerkle, A. L., and Mikhail, S. (2017). The geobiological nitrogen cycle: from microbes to the mantle. *Geobiology* 15, 343–352. doi: 10.1111/gbi.12228

Zerkle, A. L., Poulton, S. W., Newton, R. J., Mettam, C., Claire, M. W., Bekker, A., et al. (2017). Onset of the aerobic nitrogen cycle during the great oxidation event. *Nature* 542, 465–467. doi: 10.1038/nature20826

Zhang, X., Sigman, D. M., Morel, F. M., and Kraepiel, A. M. (2014). Nitrogen isotope fractionation by alternative nitrogenases and past ocean anoxia. *Proc. Natl. Acad. Sci. U.S.A.* 111, 4782–4787. doi: 10.1073/pnas.1402976111

Zhong, R., Brugger, J., Chen, Y., and Li, W. (2015). Contrasting regimes of Cu, Zn and Pb transport in ore-forming hydrothermal fluids. *Chem. Geol.* 395, 154–164. doi: 10.1016/j.chemgeo.2014.12.008

Conflict of Interest: The authors declare that the research was conducted in the absence of any commercial or financial relationships that could be construed as a potential conflict of interest.